Soft Matter

PAPER

View Article Online
View Journal | View Issue

Cite this: *Soft Matter*, 2016, **12**, 3972

Molecular dynamics simulations of uniaxial deformation of thermoplastic polyimides†

V. M. Nazarychev,[a] A. V. Lyulin,[b] S. V. Larin,[a] A. A. Gurtovenko,[ac] J. M. Kenny[ad] and S. V. Lyulin*[ac]

The results of atomistic molecular-dynamics simulations of mechanical properties of heterocyclic polymer subjected to uniaxial deformation are reported. A new amorphous thermoplastic polyimide R–BAPO with a repeat unit consisting of dianhydride 1,3-bis-(3′,4,-dicarboxyphenoxy)diphenyl (dianhydride R) and diamine 4,4′-bis-(4″-aminophenoxy)diphenyloxide (diamine BAPO) was chosen for the simulations. Our primary goal was to establish the impact of various factors (sample preparation method, molecular mass, and cooling and deformation rates) on the elasticity modulus. In particular, we found that the elasticity modulus was only slightly affected by the degree of equilibration, the molecular mass and the size of the simulation box. This is most likely due to the fact that the main contribution to the elasticity modulus is from processes on scales smaller than the entanglement length. Essentially, our simulations reproduce the logarithmic dependence of the elasticity modulus on cooling and deformation rates, which is normally observed in experiments. With the use of the temperature dependence analysis of the elasticity modulus we determined the flow temperature of R–BAPO to be 580 K in line with the experimental data available. Furthermore, we found that the application of high external pressure to the polymer sample during uniaxial deformation can improve the mechanical properties of the polyimide. Overall, the results of our simulations clearly demonstrate that atomistic molecular-dynamics simulations represent a powerful and accurate tool for studying the mechanical properties of heterocyclic polymers and can therefore be useful for the virtual design of new materials, thereby supporting cost-effective synthesis and experimental research.

Received 28th January 2016,
Accepted 16th March 2016

DOI: 10.1039/c6sm00230g

www.rsc.org/softmatter

Introduction

Polyimides (PI) are heat-resistant polymers that are widely used in aircraft, airspace and mechanical engineering as all-purpose materials that can provide efficient performance under extreme environmental conditions and long-lasting load without significant degradation of their properties.[1,2] Scientific interest in heat-resistant polymers, in general, and in aromatic polyimides, in particular, is also due to the fact that incorporation of some "hinge" groups (heteroatoms of oxygen, sulfur, sulfone group, *etc.*) into the repeat unit of a polymer chain can successfully be used to synthesize new thermoplastic polymers.[1,2] Such polyimides and polyimide-based materials show both good mechanical properties[3–12] and substantial resistance to high temperatures, chemicals and increased radiation levels.[13]

However, due to the complex chemical structure of the diamine and dianhydride fragments of PI repeat units, the relationship between the chemical composition of the thermoplastic polyimides and their mechanical properties remains unclear.[13] Furthermore, due to their complex chemical structure, the thermoplastic polyimides may show relatively low local translational and rotational mobilities of polymer chain fragments, in contrast to those observed for commodity polymers, such as polyethylene or polystyrene. Overall, these features can lead to specific changes in the relaxation patterns of different fragments of repeat units of thermoplastic polyimides subjected to an external deformation field. They can also significantly affect the correlation between their mechanical properties and temperature, pressure and other external factors, as compared to the corresponding correlations seen for polymers of simpler chemical structure.

Therefore, the synthesis of new polyimides requires large-scale experimental research, including an analysis of the effects of temperature and external pressure. Unfortunately, such experimental studies are quite resource-intensive.[1,2] That is why

[a] *Institute of Macromolecular Compounds, Russian Academy of Sciences, Bol'shoi pr. 31 (V.O.), St. Petersburg, 199004, Russia. E-mail: s.v.lyulin@gmail.com*
[b] *Theory of Polymers and Soft Matter Group, Technische Universiteit Eindhoven, PO Box 513, 5600 MB Eindhoven, The Netherlands*
[c] *Faculty of Physics, St. Petersburg State University, Ul'yanovskaya str. 1, Petrodvorets, St. Petersburg, 198504, Russia*
[d] *Materials Science and Technology Centre, University of Perugia, Loc. Pentima, 4, 05100 Terni, Italy*

† Electronic supplementary information (ESI) available. See DOI: 10.1039/c6sm00230g

computer simulation techniques used along with fully-atomistic computational models, are regarded as efficient and much cheaper methods for the comparative study of mechanical properties of new thermoplastic polyimides.

As far as the computer simulations of mechanical properties of polymers are concerned, it is still not clear how to correctly account for the influence of the thermal history (cooling rate[14–16]) and the load application rate (deformation rate[17–29]). Our study will focus exactly on these two issues, namely the sensitivity of the elasticity modulus to the cooling and deformation rates employed in simulations. This will allow us to determine the optimal values of the cooling and deformation rates to be used in simulations in order to appropriately model the thermomechanics of thermoplastic polyimides.

The next section of the paper focuses on the polymer materials in question and the simulation details, as well as on the uniaxial deformation strategy. The effects of the degree of equilibration, cooling and deformation rates, the molecular mass and the size of a periodic simulation cell on the elasticity modulus are studied in the subsequent sections of the paper. Finally, the influence of the temperature and external pressure on mechanical properties of the thermoplastic polyimides is reported and discussed.

Materials

Thermoplastic polyimide R–BAPO

The thermal properties of tetranuclear aromatic thermoplastic polyimides[30–32] based on a dianhydride 1,3-bis-(3′,4,-dicarboxyphenoxy)diphenyl (dianhydride R) were investigated in our previous studies,[33–36] while their mechanical properties were not studied computationally so far. To explore their mechanical properties we chose the polyimide R–BAPO[36,37] (based on dianhydride R and a diamine 4,4′-bis-(4″-aminophenoxy)diphenyloxide (diamine BAPO)) which was recently synthesized in the Institute of Macromolecular Compounds, Russian Academy of Sciences, see Fig. 1.

Comparing three previously considered thermoplastic polyimides (R–BAPS, R–BAPB and R–BAPO),[33–36] the choice of PI R–BAPO for studying the mechanical properties can mainly be justified by the following two reasons. First, in contrast to the partially crystallizing PI R–BAPB, the polyimide R–BAPO is fully amorphous, which allows us to rule out completely the effects related to the crystallization processes and investigate the mechanical properties of a fully amorphous polymer sample. Second, PI R–BAPO is characterized by a negligible anisotropy in the distribution of partial charges. This is in drastic contrast to PI R–BAPS, whose repeat unit contains a highly polar sulfone group that creates additional computational issues.

Methods

Simulation protocol

The simulation details related to the preparation of the equilibrated configuration can be found in our previous publications on the subject.[33–36] Shortly, to generate the initial configuration, 27 polymeric chains with the degree of polymerization N_p = 8 in the ''polymer gas'' state were compressed. After the compression step the pressure was reduced to 1 atm. To relieve the remaining residual stress, a cyclic annealing procedure was performed within the temperature range from 600 K to 300 K. The annealing was followed by equilibration for 2 μs at T = 600 K. Standard checks[36] were used to prove that the equilibrium state has been reached. After that, a 1 μs production simulation was performed; instantaneous configurations of the system being saved every 100 ns. The selected 11 instantaneous states were used as initial states for the cooling procedure.

The polymer samples were then cooled down to temperature of 290 K. In order to examine the influence of the simulated cooling rate γ_c on the mechanical properties, a cooling procedure was applied with five different values of γ_c, spanning the range from 1.5×10^{10} K min^{-1} to 1.5×10^{14} K min^{-1}.

In order to reduce the required simulation time, we do not take into account the electrostatic interactions (EI)[35] in the present study. Such an assumption is justified due to the rather small contribution of EI energy of PI R–BAPO to the total potential energy ($\sim$25%),[36] electrostatic interactions do modify the mechanical properties of PI R–BAPO but do not change the qualitative conclusions of the present study. Similar simulations without explicit EI are widely used in studies that dealt with polyimide mechanical properties;[38–40] the possible influence of EI will be discussed in our future publication.

After the cooling step, each of the prepared 11 samples has been deformed with a stretching rate γ_d that was varied in the range from 10^{-1} nm ps^{-1} to 10^{-5} nm ps^{-1}. For a periodic simulation cell of length of $\sim$5.8 nm, the corresponding deformation rate amounted to $1.8 \times (10^6$–$10^{10})$ s^{-1}. The simulations have been performed using the molecular-dynamics (MD) package Gromacs 4.5.6[41,42] and the force field Gromos53a5.[43] All simulations required $\sim$1.6 million processor hours and were performed using 64 cores on Lomonosov (Intel Xeon X5570 CPUs) and Chebyshev (Intel Xeon E5472 CPUs) supercomputers at Moscow State University.

Simulation of mechanical properties

As mentioned above, the polymer samples were first cooled down to T = 290 K. This temperature is substantially lower than the glass-transition value of $T_g \sim$ 460–470 K[36] measured in

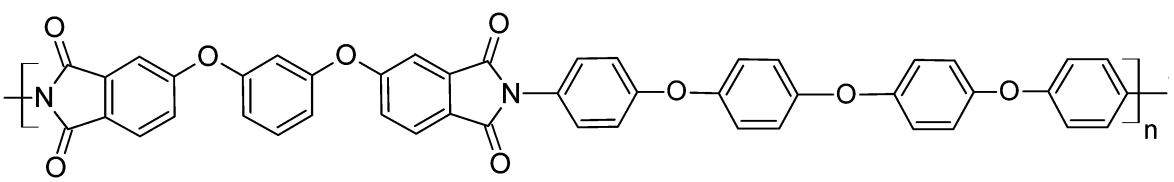

Fig. 1 Chemical structure of a repeat unit of the thermoplastic PI R–BAPO.

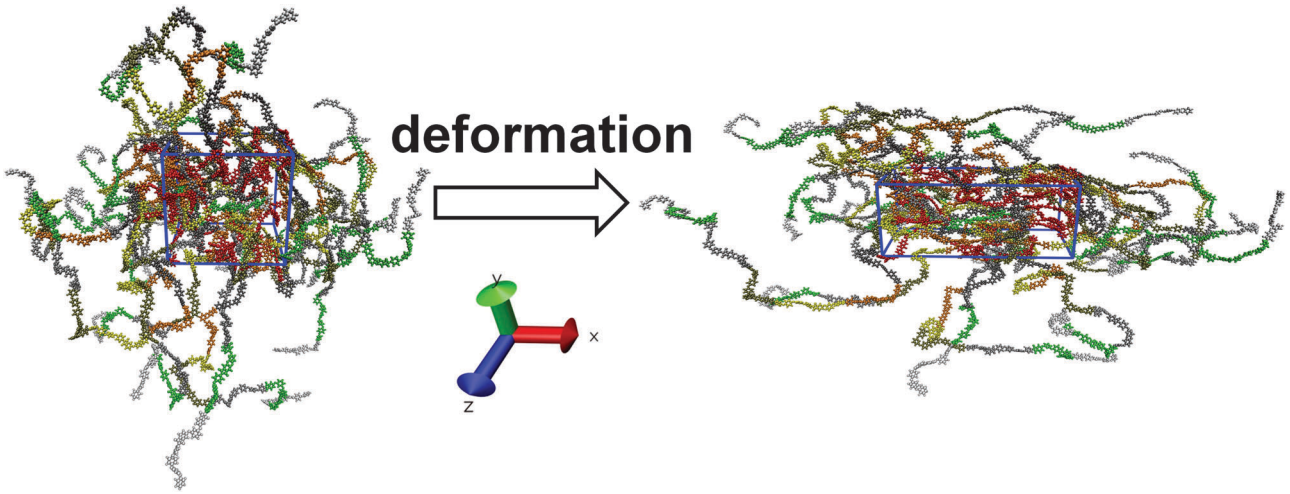

Fig. 2 PI R–BAPO sample configuration before (left) and after (right) uniaxial deformation along the *X* axis. The periodic cell is highlighted in blue.

simulations of similar polyimides without EI. After cooling, the samples were subjected to uniaxial deformation following the deformation protocol proposed elsewhere for calculating the stress–strain dependences.[44] Prior to the deformation, the LINCS algorithm[45] that keeps the length of chemical bonds constant was disabled and the chemical bonds were described with the use of the harmonic potential from the same force field. After that, the simulated systems were additionally equilibrated for 400 ps. The LINCS algorithm had to be disabled due to the observed instability of simulations on a multi-processor system upon high-speed deformation. The density change after the LINCS deactivation did not exceed 1.5%.

The uniaxial deformation changes the periodic cell size at a constant rate, along the positive direction of one of the reference axes – *X*, *Y* or *Z* –[44] so that the isotropic Berendsen barostat[46] with a time constant $\tau_p = 0.5$ ps was replaced with the anisotropic Berendsen barostat with $\tau_p = 1$ ps. In the direction of the applied deformation the samples remained incompressible, *i.e.* the compressibility of the system in this direction was set to zero. In the transverse direction the system compressibility was set to 4.5×10^{-10} Pa^{-1}. Therefore, upon stretching a simulation cell elongates in the direction of deformation and compresses in the directions transversal to deformation in response to the external pressure (1 bar), see Fig. 2.

During deformation the values of the pressure tensor P_i, $i = x, y, z$, and the simulation cell size L_i in the stretching direction were saved each 1 ps. The characteristics obtained were converted to the dependence of the stress σ on the relative strain ε as[47]

$$\sigma = -P_i,$$
$$\varepsilon = (L_i - L_{0i})/L_{0i}, \quad (1)$$

where L_{0i} is the simulation cell size prior to the deformation ($t = 0$). The initial part of the dependence $\sigma(\varepsilon)$ shows a linear regime up to ~2% of the deformation ε, and the elastic modulus E is defined as

$$\sigma = E\varepsilon. \quad (2)$$

The value of E was determined as the slope of the linearly approximated dependence $\sigma(\varepsilon)$ in the linear viscoelasticity regime. It should be emphasized that, in some cases, the sample had initial residual stress, meaning that the dependence $\sigma(\varepsilon)$ does not always emerge from zero. To calculate the value of the modulus E in this case, the dependence $\sigma(\varepsilon)$ was simply shifted. The error bars in elasticity modulus calculations were computed as mean-square deviations from the average value $\bar{E}$, obtained by averaging over all samples and three deformation directions, $i = x, y, z$.

Elastic properties can also be analyzed with the transversal dimensions fixed during the deformation.[48] The value of the modulus determined in this way combines the Young's modulus E and the polymer bulk modulus, and differs from the elasticity modulus calculated using the present approach.

The yield peak σ_y (the onset of plastic deformation in the material) and the strain-hardening modulus G_h (the slope of the linear dependence $\sigma(\varepsilon)$ in the post-yield deformation regime) were calculated as[49–52]

$$\sigma = \sigma_y + G_h(\lambda^2 - \lambda^{-1}). \quad (3)$$

To this end, the dependence $\sigma(\varepsilon)$ was converted from the engineering strain function ($\varepsilon = \lambda - 1$) to the strain dependence ($\varepsilon_t = \lambda^2 - \lambda^{-1}$), where $\lambda = L_i/L_{0i}$. Eqn (3) is used to calculate the so-called offset yield peak which is slightly lower than the yield peak value determined in experiment.[49]

Results

Influence of the degree of equilibration, cooling and deformation rates

The influence of the degree of equilibration. Well-equilibrated samples obtained in long-running simulations of ~3 μs have been used to investigate the influence of the degree of equilibration on the mechanical properties in the glassy state (see ESI†). Overall, we found that the values of

the modulus E are very weakly affected by the degree of equilibration, see ESI† and Fig. S1, ESI.† The final results fluctuate around the mean value of $E = 2.7 \pm 0.3$ GPa.

Such behaviour of Young's modulus dependence on the degree of equilibration can be due to the preliminary annealing, where some equilibration of the samples in the glassy state has been done. This equilibration led to the rather weak dependence on the sample thermal history. Thus it might be sufficient for the accurate calculation of the mechanical properties in the present molecular-dynamics simulations.

Our findings also show that the modulus of elasticity for well-equilibrated polymer samples (Fig. S2 and Table S1, ESI†) hardly depends on their molecular mass (Fig. S3 and S4, ESI†). The dependence of mechanical properties on the size of a periodic simulation cell was examined as well, and no sufficient influence was observed (Table S2 and Fig. S5, ESI†). Such insensitivity of the elastic modulus is due to the fact that the modulus is mainly determined by the processes on the scales that do not exceed the entanglement length.

The influence of the cooling rate (thermal history). It is well known that polymer samples with different thermal history may show different mechanical properties.[14,15,53] In the experiments, the cooling of polymer melts is performed at rates 10–11 orders of magnitude slower than in typical MD simulations. Such a significant difference between the experimental and computational cooling rates may limit the number of relaxation processes which could be activated within typical simulation times, as compared to those in physical experiments. As a result, it can affect the shape of the energy landscape in the polymer glass in simulations and influence the values of major macroscopic material properties such as density and intramolecular energy.

After switching off the LINCS algorithm, the samples obtained by cooling with five different rates γ_c from 1.5×10^{10} K min^{-1} to 1.5×10^{14} K min^{-1} were deformed at a stretching rate $\gamma_d = 1.8 \times 10^{8}$ s^{-1}, see Fig. 3a. The results show that the extracted values of the modulus E depend logarithmically on the cooling rate γ_c, see Fig. 3b.

The logarithmic relationship between the elasticity modulus and the cooling rate is known from experimental studies on polyheteroarylenes.[53] A similar dependence was also reported for a simple two-dimensional model of an amorphous glass.[14] To the best of our knowledge, such a logarithmic dependence has never been observed in atomistic computer simulations of thermoplastic polyimides.

Such mechanical behavior of the PI samples with different thermal history is likely to be determined by both differences in the density at room temperature,[49] see Fig. 4a, and different values of the typical intramolecular energy of excluded-volume interactions, see Fig. 4b.

As the cooling rate γ_c decreases, the density of a sample in the glassy state systematically increases, leading to an increase in the number of contacts between polymer chains and a drop in the free volume. In the strain-hardening regime the dependences $\rho(\varepsilon)$ that are calculated for various values of γ_c reach some constant density, see Fig. 4a. A similar behavior is observed for the strain dependence of the energy of excluded volume interactions, see Fig. 4b, where the saturation becomes clearly visible for deformations that exceed 20%. This is a manifestation of mechanical rejuvenation or (at least in part) of the removal of the thermal history upon deformation.[54,55]

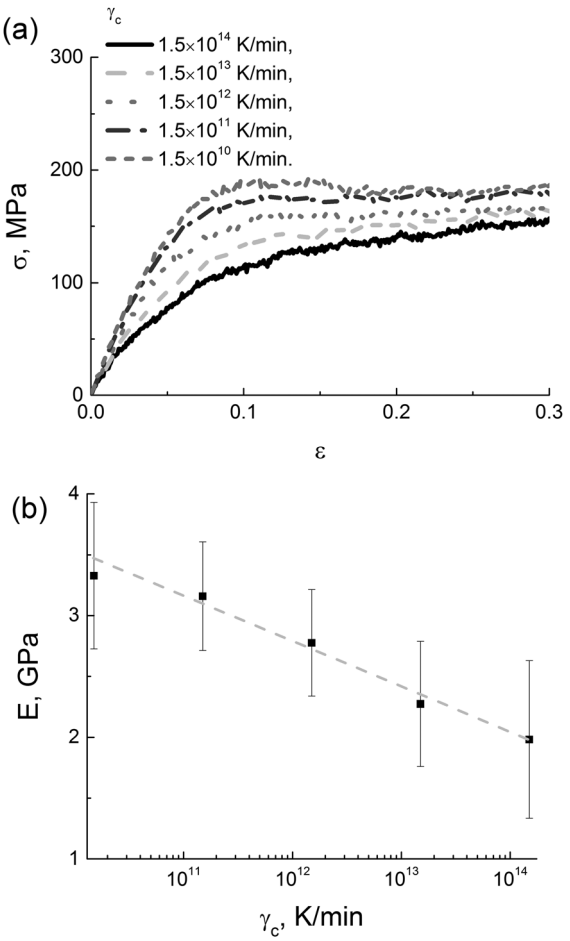

Fig. 3 (a) Stress–strain dependences for different values of γ_c and (b) cooling-rate dependence of the elastic modulus in simulations; the logarithmic fit is shown by the dotted line.

The influence of the deformation rate. To investigate the influence of the deformation rate γ_d on the elasticity modulus, the samples of PI R–BAPO have been cooled down with a cooling rate of $\gamma_c = 1.5 \times 10^{12}$ K min^{-1}, and were further deformed with different deformation rates γ_d from 1.8×10^{6} s^{-1} to 1.8×10^{10} s^{-1}, see Fig. 5a. The resulting strain-rate dependence $E(\gamma_d)$ is very close to the logarithmic one, see Fig. 5b.

The results obtained for PI R–BAPO confirm the logarithmic dependence $E(\gamma_d)$ observed previously in coarse-grained simulations of polyethylene and polypropylene[21,56] and also in experimental studies of various polymers and composite polymer-based materials.[57,58]

It is noteworthy that for the samples with very high deformation rates that exceed $\gamma_d = 1.8 \times 10^{10}$ s^{-1} ($\sim$100 m s^{-1}) and approach acoustic velocities, the dependence $E(\gamma_d)$ clearly deviates from the logarithmic behavior, see Fig. 5b. Coarse-grained simulations of polyethylene demonstrated that the elasticity modulus

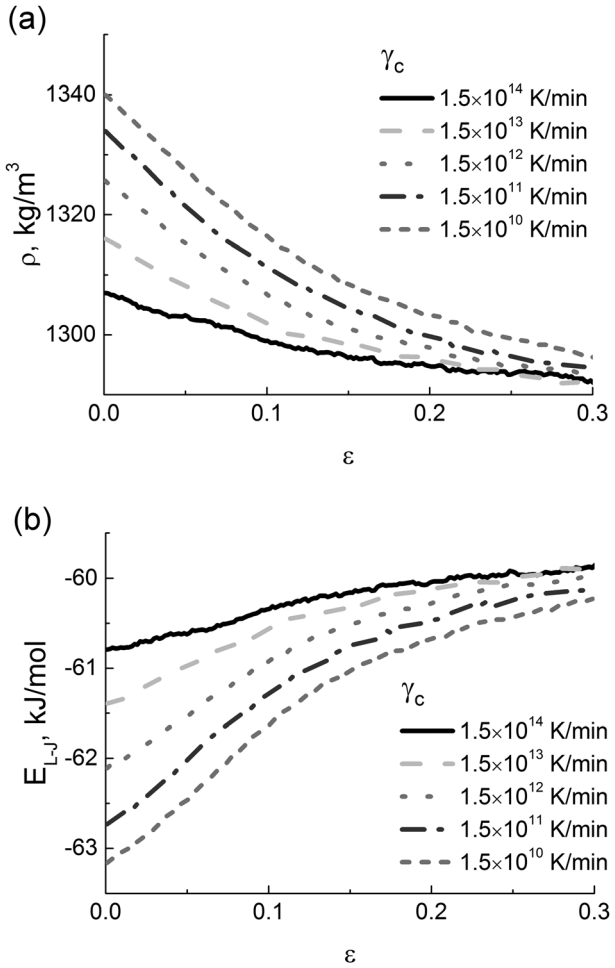

Fig. 4 (a) Strain dependence of the PI density and (b) energy of excluded-volume interactions ($E_{L\text{-}J}$) at various cooling rates γ_c.

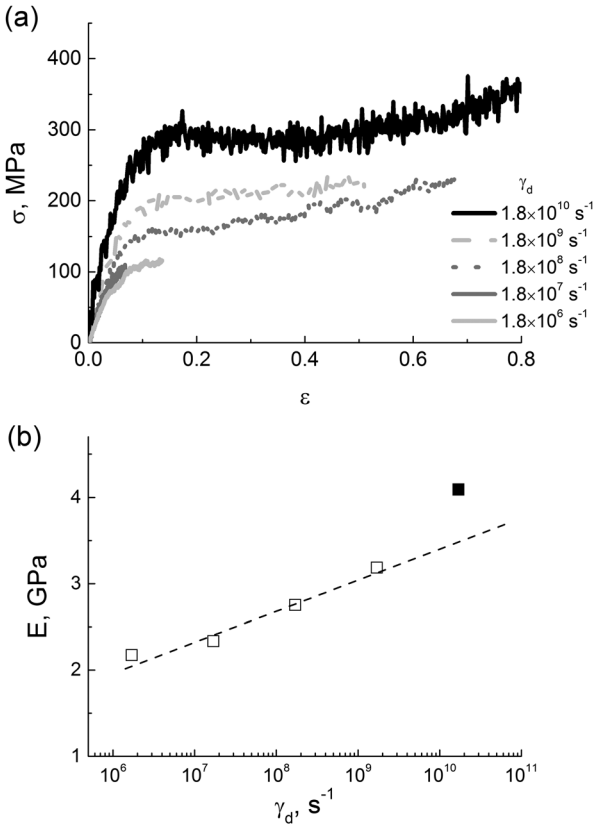

Fig. 5 (a) PI R–BAPO stress–strain dependences for different deformation rates γ_d and (b) the modulus $E(\gamma_d)$ as a function of the deformation rate γ_d; the logarithmic fit is shown by the dotted line. The filled square shows that the elasticity modulus clearly deviates from the logarithmic dependence for the deformation with the highest simulated rate, $\gamma_d = 1.8 \times 10^{10}$ s^{-1}.

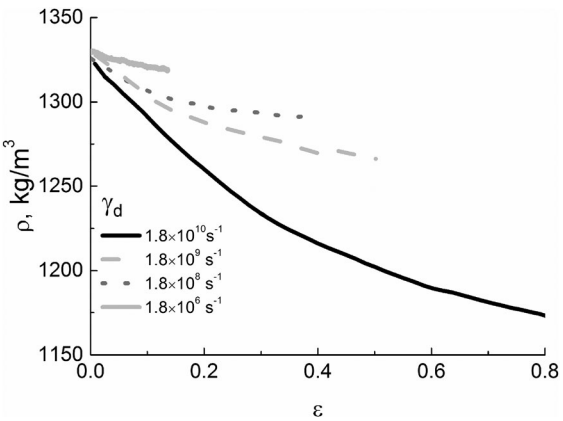

Fig. 6 The PI R–BAPO density $\rho(\varepsilon)$ as a function of the relative strain for different values of γ_d.

also deviated from the logarithmic dependence[21] at even higher rates (as high as 10^{11} s^{-1}).

Some possible explanations for the observed non-logarithmic dependence of the elasticity modulus on the deformation rate can be linked to the presence of additional sub-T_g relaxation processes that are activated in polymer glasses under fast deformation. At high stretching rates the polymer internal structure undergoes substantial changes that are manifested in a rather rapid density drop, even in the linear viscoelastic regime (relative deformation of a few percent), see Fig. 6.

Thus, we can conclude that a correct choice of deformation-rate values in atomistic computer simulations is important for determining the mechanical properties of thermoplastic polyimides and for a subsequent comparison with experimental data. In the following the values of the deformation were taken below 1.8×10^9 s^{-1}, *i.e.* well within the logarithmic regime of $E(\gamma_d)$ dependence.

Influence of temperature and external pressure on mechanical properties

To get an insight into the performance range of thermoplastic PIs, it is essential to explore the impact of temperature and external pressure on their mechanical properties.

The influence of temperature on mechanical properties. In simulations we calculated the mechanical characteristics of the thermoplastic PI R–BAPO both at temperatures above and below the glass-transition temperature T_g. To this end, instant polymer configurations were saved during the cooling procedure from 600 K to 290 K, which was performed at a cooling rate of $\gamma_c = 1.5 \times 10^{12}$ K min^{-1}. During the cooling, the

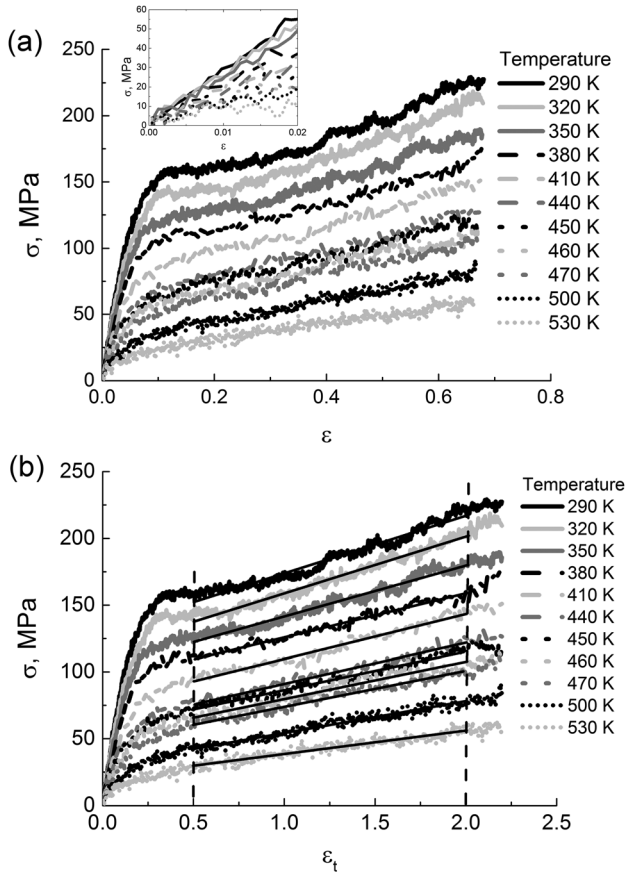

Fig. 7 (a) The stress in PI R–BAPO samples as a function of the engineering strain ε at different temperatures. The inset shows the linear viscoelastic regime. (b) The stress in PI R–BAPO samples as a function of the strain ε_t at different temperatures. Solid black lines indicate the linear fits in the strain-hardening regime as highlighted by the vertical dotted lines, see eqn (3).

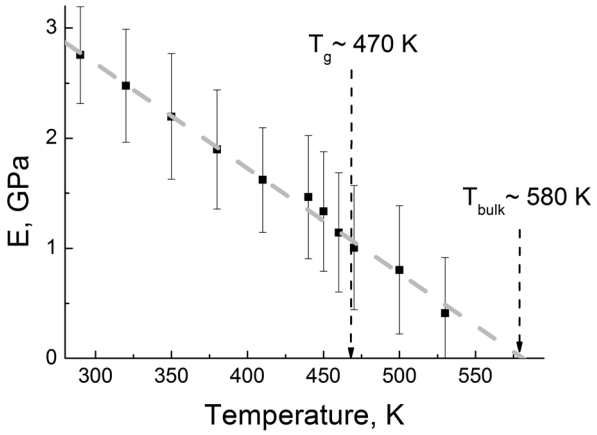

Fig. 8 The elasticity modulus as a function of temperature. A dashed grey line corresponds to the linear fit. Dashed arrows indicate T_{bulk} (E equals zero at T_{bulk}) and T_g of R–BAPO PI as estimated previously.[36]

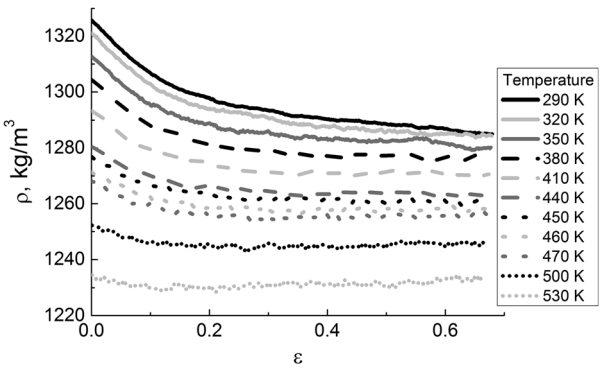

Fig. 9 Density–strain dependences for PI R–BAPO at various temperatures.

PI R–BAPO samples were deformed at each intermediate temperature with a deformation rate $\gamma_d = 1.8 \times 10^8$ s^{-1}. Fig. 7a shows the resulting dependences $\sigma(\varepsilon)$ on the engineering strain ε, while Fig. 7b presents the stress–strain $\sigma(\lambda^2 - \lambda^{-1})$ relationships, where $\lambda = L/L_0$.

The initial part of the $\sigma(\varepsilon)$ dependence at different temperatures was used for calculating the temperature dependence $E(T)$ of the elasticity modulus, see Fig. 8.

The analysis of the data in Fig. 8 shows that the modulus drops almost linearly with temperature. Similar dependences $E(T)$ were also found in other simulation studies,[21,59] and they were also qualitatively confirmed by experimental data.[60,61]

When temperature approaches T_g from the low-temperature region, the value of E decreases by $\sim$45% as compared to the E value at room temperature. Extrapolation of the dependence $E(T)$ to zero gives the flow temperature of $T_{bulk} \sim 580$ K; this corresponds to the temperature at which the highly elastic response of the material to the applied load changes to a viscous flow. One can therefore conclude that the temperature $T = 600$ K that was selected for the equilibration stage corresponds to highly-mobile PI melt conditions.

The temperature range of the viscoelasticity for the majority of polymers is determined by their chemical structure. For thermoplastic PIs the highly-elastic state can be maintained in a rather broad temperature range from room temperature to temperatures that exceed by $\sim$100 K the glass transition temperature $T_g = 470$ K.[36]

We also analyzed the density–strain dependences at different temperatures, see Fig. 9.

During deformation, the density decreases until a T-dependent constant value is reached at different strain values. The combined influence of temperature and deformation rate makes the sample plastic at lower values of ε when temperature increases. The state of viscous flow defines the material reaction to external pressure, and the polymer liquid becomes practically incompressible under such conditions. Note that we did not observe any significant increase in the density and the magnitude of (negative) excluded volume (LJ). The deformation above T_g has to be done with caution, due to the large fluctuations of these characteristics. To obtain reliable results, the number of simulated samples should be large enough to provide good statistics. The results obtained are in line with the simulation findings for mechanical properties of commodity polymers.[44,59]

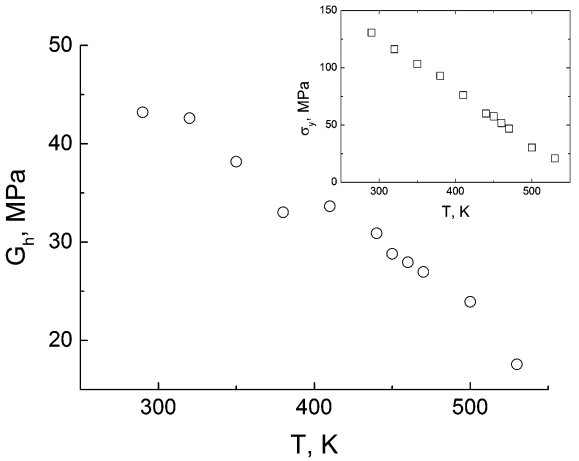

Fig. 10 Temperature dependence of the strain-hardening modulus. The inset shows the temperature dependence of the yield peak. The error bars are smaller than the symbol size.

With temperature the yield peak and the strain-hardening modulus decrease,[62] see Fig. 10.

The analysis of the results presented in Fig. 10 shows that both the yield peak and the strain-hardening modulus decrease almost linearly as temperature increases. In the case of the yield peak dependence such behavior is in good agreement with other computer simulations.[44] The theory of rubbery elasticity predicts that the strain-hardening modulus (G_h) should increase with temperature,

$$G_h = k_B T\rho/M_e \quad (4)$$

where ρ is the polymer density and M_e is the entanglement molecular weight. However, the results of both experimental studies and previous computer simulations[49] as well as our present data imply that the G_h values decrease with temperature in agreement with some recent findings.[62]

The influence of external pressure on mechanical properties. We now turn to the performance of PI R–BAPO under a constant load and additional external pressure. The cooled samples of R–BAPO ($\gamma_c = 1.5 \times 10^{12}$ K min^{-1}) at $T = 290$ K were compressed isotropically at external pressure that was varied from 50 MPa to 500 MPa. During the uniaxial stretching with $\gamma_d = 1.8 \times 10^8$ s^{-1} the external pressure was maintained constant with the use of the Berendsen barostat, see Fig. 11.

The modulus increases linearly with external pressure P from 2.7 GPa ($P = 0$) to ~3.7 GPa ($P = 500$ MPa), see Fig. 12.

The results obtained are qualitatively supported by experimental data for commodity polymers.[63,64] To the best of our knowledge, the influence of the external pressure on mechanical properties of polyimides has not been reported yet.

The values of the yield peak σ_y and the strain-hardening modulus G_h also depend on the amount of the applied external pressure, see Fig. 13. With the increase of pressure both σ_y and G_h linearly increase. This correlation was established for the first time in simulations of atactic polystyrene under external pressure.[49] Our findings in Fig. 13 are qualitatively supported by experimental data for other polymers.[28,63,64] It is known that

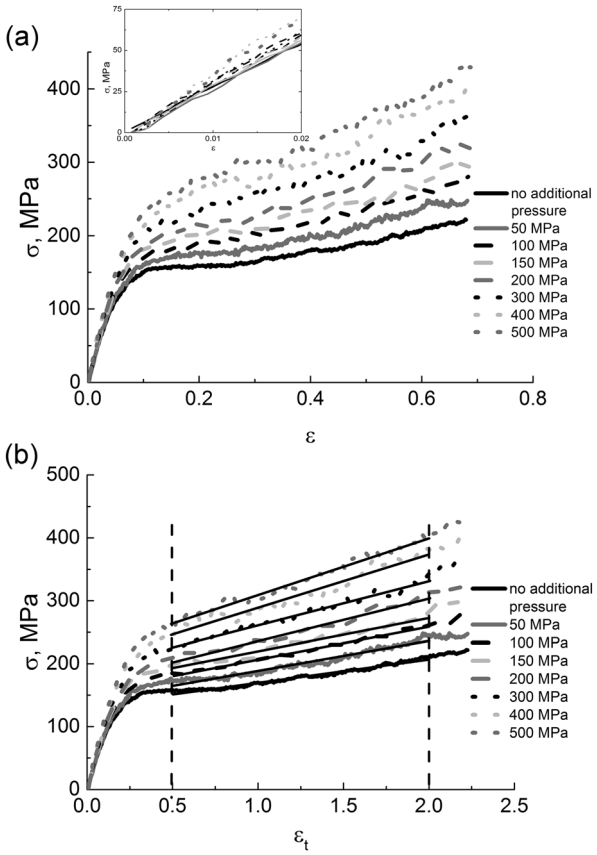

Fig. 11 (a) The stress of PI R–BAPO samples under external pressure as a function of the engineering strain ε at $T = 290$ K. The inset shows the linear viscoelasticity regime. (b) The stress of PI R–BAPO samples under external pressure as a function of the strain ε_t at $T = 290$ K. Solid black lines are linear fits in the strain-hardening regime that is defined by the vertical dashed lines.

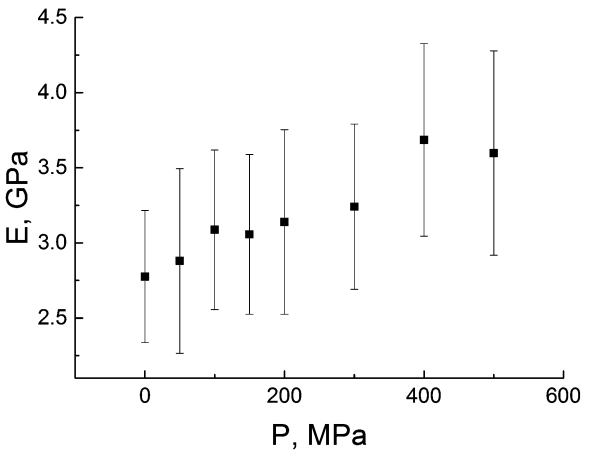

Fig. 12 The PI R–BAPO elasticity modulus as a function of external pressure.

the ratio G_h/σ_y may act as an empirical relation that describes the strength of the polymer material[49,50] (the so-called Considere criterion), which is often related to the neck formation as a result of the deformation when $G_h/\sigma_y < 1/3$. As G_h/σ_y exceeds

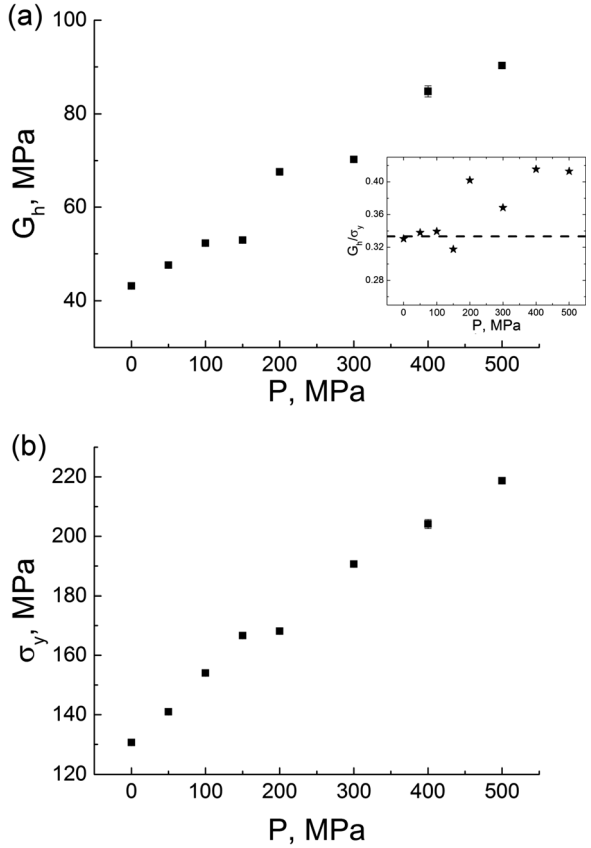

Fig. 13 (a) The PI R–BAPO strain-hardening modulus as a function of external pressure applied. The inset shows the G_h/σ_y as a function of the external pressure. The dashed line in the inset corresponds to Considere's criterion that determines the strength performance of the material. (b) The yield peak as a function of external pressure.

1/3, the material strength is supposed to increase. The dependence G_h/σ_y on external pressure at $T = 290$ K clearly distinguishes two regimes: G_h/σ_y is approximately equal to 1/3 under an external pressure of ≤ 200 MPa, and is above 1/3 under an external pressure of > 200 MPa. Such behavior is likely to be associated with the substantial increase in the material strength under certain values of external pressure.

Summarizing, the application of external pressure has a significant impact on practically all investigated mechanical properties, leading to a considerable increase in the elasticity modulus, the yield peak and the strain-hardening modulus. The strength of thermoplastic PI R–BAPO can be controlled by changing the external pressure; this property can be used to create new high-performance materials.

Conclusions

In this paper we employed atomic-scale molecular dynamics simulations to explore the mechanical properties of a novel thermoplastic polyimide R–BAPO under uniaxial deformation. The influence of various factors (cooling and deformation rates, external temperature and pressure) on the mechanical properties was extensively studied. It was demonstrated that the elasticity modulus is practically independent of the molecular mass, the size of the simulation box, and the degree of equilibration of the polymer sample. The simulations reported here successfully reproduce the well-known logarithmic dependence of the elasticity modulus on the cooling and deformation rates. It was established that the uniaxial stretching of PI samples with different thermal history leads to significant changes in the density and the energy of excluded-volume interactions during deformation. At the initial deformation stage, these values are determined by the material thermal history. Yet, as the deformation exceeds the yield strain, the dependences of both the density and the energy of excluded-volume interactions for the samples with different thermal history reach the same values; this effect can be interpreted as mechanical rejuvenation.

The dependence of the elasticity modulus on the deformation in the acoustic regime ($\sim 10^{10}$ s^{-1}) deviates from the logarithmic dependence observed at much lower deformation rates (in both simulations and experiments). These findings most likely can be related to the thermally-activated nature of the polymer glass deformation due to the possible additional contributions of fast sub-T_g relaxation processes that are activated at high deformation rates.

Extrapolation of the T-dependence of the elasticity modulus to the zero modulus value was used to determine the temperature of transition from the highly elastic state to the viscous-flow state, $T_{bulk} \sim 580$ K. Simulations showed the linear dependence of the yield peak and the strain hardening modulus on external pressure in agreement with previously obtained data.[49] We also found an almost linear dependence of these characteristics on temperature. Our computational results also showed an increase in higher strength performance of R–BAPO with temperature (for temperatures below the glass transition temperature). Applying high external pressure (200 MPa and above) at a temperature of 290 K may lead to a further improvement of PI strength.

Overall, our study clearly demonstrates the ability of the state-of-the-art atomic-scale MD simulations to appropriately describe the mechanical properties of heterocyclic polymers. The developed protocols will be used in the nearest future for a comparative study of mechanical properties of composite materials based on these thermoplastic polyimides, which are reinforced with carbon nanofillers of various shapes and sizes.

Acknowledgements

This study was supported by the Russian Ministry of Education and Science within the State Contract No. 14.Z50.31.0002 (Megagrant). The simulations were performed using the computational resources of the Institute of Macromolecular Compounds, Russian Academy of Sciences, and the Chebyshev and Lomonosov supercomputers at Moscow State University.

References

1 M. I. Bessonov, M. M. Koton, V. V. Kudryavtsev and L. A. Laius, *Polyimides: Thermally Stable Polymers*, Plenum, New York, NY, 1987.
2 M. Ghosh, *Polyimides: Fundamentals and Applications*, CRC Press, 1996.
3 A. S. Argon and M. I. Bessonov, *Philos. Mag.*, 1977, **35**, 917–933.
4 J. W. Kang, K. Choi, W. H. Jo and S. L. Hsu, *Polymer*, 1998, **39**, 7079–7087.
5 J. Huang, C. He, Y. Xiao, K. Y. Mya, J. Dai and Y. P. Siow, *Polymer*, 2003, **44**, 4491–4499.
6 V. E. Smirnova, I. V. Gofman, E. M. Ivan'kova, A. L. Didenko, A. V. Krestinin, G. I. Zvereva, V. M. Svetlichnyi and V. E. Yudin, *Polym. Sci., Ser. A*, 2013, **55**, 268–278.
7 I. V. Gofman, V. E. Yudin, O. Orell, J. Vuorinen, A. Y. Grigoriev and V. M. Svetlichnyi, *J. Macromol. Sci., Part B: Phys.*, 2013, **52**, 1848–1860.
8 M. Yoonessi, Y. Shi, D. A. Scheiman, M. Lebron-Colon, D. M. Tigelaar, R. A. Weiss and M. A. Meador, *ACS Nano*, 2012, **6**, 7644–7655.
9 D. M. Delozier, K. A. Watson, J. G. Smith, T. C. Clancy and J. W. Connell, *Macromolecules*, 2006, **39**, 1731–1739.
10 P. C. Irwin, Y. Cao, A. Bansal and L. S. Schadler, in 2003 Annual Report Conference on Electrical Insulation and Dielectric Phenomena, IEEE, 2003, pp. 120–123.
11 L.-B. Zhang, J.-Q. Wang, H.-G. Wang, Y. Xu, Z.-F. Wang, Z.-P. Li, Y.-J. Mi and S.-R. Yang, *Composites, Part A*, 2012, **43**, 1537–1545.
12 H. W. Ha, A. Choudhury, T. Kamal, D.-H. Kim and S.-Y. Park, *ACS Appl. Mater. Interfaces*, 2012, **4**, 4623–4630.
13 D.-J. Liaw, K.-L. Wang, Y.-C. Huang, K.-R. Lee, J.-Y. Lai and C.-S. Ha, *Prog. Polym. Sci.*, 2012, **37**, 907–974.
14 J. Ashwin, E. Bouchbinder and I. Procaccia, *Phys. Rev. E*, 2013, **87**, 042310.
15 Y. Shi and M. Falk, *Phys. Rev. Lett.*, 2005, **95**, 095502.
16 K. Jordens, *Polymer*, 2000, **41**, 7175–7192.
17 R. Hoy and M. Robbins, *Phys. Rev. Lett.*, 2007, **99**, 117801.
18 L. C. A. van Breemen, T. A. P. Engels, E. T. J. Klompen, D. J. A. Senden and L. E. Govaert, *J. Polym. Sci., Part B: Polym. Phys.*, 2012, **50**, 1757–1771.
19 J. Rottler and M. Robbins, *Phys. Rev. E*, 2003, **68**, 011507.
20 G. A. Medvedev, J. W. Kim and J. M. Caruthers, *Polymer*, 2013, **54**, 6599–6607.
21 I. H. Sahputra and A. T. Echtermeyer, *Modell. Simul. Mater. Sci. Eng.*, 2013, **21**, 065016.
22 E. Lerner and I. Procaccia, *Phys. Rev. E*, 2009, **80**, 026128.
23 J. Richeton, G. Schlatter, K. S. Vecchio, Y. Rémond and S. Ahzi, *Polymer*, 2005, **46**, 8194–8201.
24 F. M. Capaldi, M. C. Boyce and G. C. Rutledge, *Polymer*, 2004, **45**, 1391–1399.
25 A. D. Mulliken and M. C. Boyce, *Int. J. Solids Struct.*, 2006, **43**, 1331–1356.
26 E. M. Arruda, M. C. Boyce and R. Jayachandran, *Mech. Mater.*, 1995, **19**, 193–212.
27 G. T. Gray, W. R. Blurnenthal, C. P. Trujillo and R. W. Carpenter, *Mater. Res. Process. Sci.*, 1997, **7**, 523–528.
28 R. W. Truss, P. L. Clarke, R. A. Duckett and I. M. Ward, *J. Polym. Sci., Polym. Phys. Ed.*, 1984, **22**, 191–209.
29 K. Cao, Y. Wang and Y. Wang, *Mater. Des.*, 2012, **38**, 53–58.
30 V. E. Yudin, V. M. Svetlichnyi, A. N. Shumakov, D. G. Letenko, A. Y. Feldman and G. Marom, *Macromol. Rapid Commun.*, 2005, **26**, 885–888.
31 V. E. Yudin, G. M. Divoux, J. U. Otaigbe and V. M. Svetlichnyi, *Polymer*, 2005, **46**, 10866–10872.
32 V. E. Yudin, V. M. Svetlichnyi, A. N. Shumakov, R. Schechter, H. Harel and G. Marom, *Composites, Part A*, 2008, **39**, 85–90.
33 S. V. Lyulin, S. V. Larin, A. A. Gurtovenko, V. M. Nazarychev, S. G. Falkovich, V. E. Yudin, V. M. Svetlichnyi, I. V. Gofman and A. V. Lyulin, *Soft Matter*, 2014, **10**, 1224–1232.
34 S. V. Lyulin, A. A. Gurtovenko, S. V. Larin, V. M. Nazarychev and A. V. Lyulin, *Macromolecules*, 2013, **46**, 6357–6363.
35 S. V. Lyulin, S. V. Larin, A. A. Gurtovenko, N. V. Lukasheva, V. E. Yudin, V. M. Svetlichnyi and A. V. Lyulin, *Polym. Sci., Ser. A*, 2012, **54**, 631–643.
36 V. M. Nazarychev, S. V. Larin, A. V. Yakimansky, N. V. Lukasheva, A. A. Gurtovenko, I. V. Gofman, V. E. Yudin, V. M. Svetlichnyi, J. M. Kenny and S. V. Lyulin, *J. Polym. Sci., Part B: Polym. Phys.*, 2015, **53**, 912–923.
37 V. M. Nazarychev, S. V. Larin, N. V. Lukasheva, A. D. Glova and S. V. Lyulin, *Polym. Sci., Ser. A*, 2013, **55**, 570–576.
38 D. Qi, J. Hinkley and G. He, *Modell. Simul. Mater. Sci. Eng.*, 2005, **13**, 493–507.
39 S.-H. Tzeng and J.-L. Tsai, *J. Reinf. Plast. Compos.*, 2011, **30**, 922–931.
40 J.-S. Gao, S.-C. Shiu and J.-L. Tsai, *J. Compos. Mater.*, 2012, **47**, 449–458.
41 D. Van Der Spoel, E. Lindahl, B. Hess, G. Groenhof, A. E. Mark and H. J. C. Berendsen, *J. Comput. Chem.*, 2005, **26**, 1701–1718.
42 B. Hess, S. Uppsala and E. Lindahl, *J. Chem. Theory Comput.*, 2008, **4**, 435–447.
43 C. Oostenbrink, A. Villa, A. E. Mark and W. F. van Gunsteren, *J. Comput. Chem.*, 2004, **25**, 1656–1676.
44 A. V. Lyulin, N. K. Balabaev, M. A. Mazo and M. A. J. Michels, *Macromolecules*, 2004, **37**, 8785–8793.
45 B. Hess, H. Bekker, H. J. C. Berendsen and J. G. E. M. Fraaije, *J. Comput. Chem.*, 1997, **18**, 1463–1472.
46 H. J. C. Berendsen, J. P. M. Postma, W. F. van Gunsteren, A. DiNola and J. R. Haak, *J. Chem. Phys.*, 1984, **81**, 3684–3690.
47 I. M. Ward and J. Sweeney, *Mechanical Properties of Solid Polymers*, John Wiley & Sons, Ltd, Chichester, UK, 2012.
48 C. Batistakis, M. A. J. Michels and A. V. Lyulin, *Macromolecules*, 2014, **47**, 4690–4703.
49 B. Vorselaars, A. V. Lyulin and M. A. J. Michels, *J. Chem. Phys.*, 2009, **130**, 074905.
50 R. N. Haward, *Polymer*, 1994, **35**, 3858–3862.
51 R. S. Hoy, *J. Polym. Sci., Part B: Polym. Phys.*, 2011, **49**, 979–984.
52 D. J. A. Senden, J. A. W. Van Dommelen and L. E. Govaert, *J. Polym. Sci., Part B: Polym. Phys.*, 2010, **48**, 1483–1494.

53 J. E. Lincoln, R. J. Morgan and E. E. Shin, *J. Polym. Sci., Part B: Polym. Phys.*, 2001, **39**, 2947–2959.
54 A. V. Lyulin and M. A. J. Michels, *Phys. Rev. Lett.*, 2007, **99**, 085504.
55 H. G. H. van Melick, L. E. Govaert and H. E. H. Meijer, *Polymer*, 2003, **44**, 3579–3591.
56 H. Mae, M. Omiya and K. Kishimoto, *Trans. Japan Soc. Comput. Methods Eng.*, 2008, **7**, 6–11.
57 G. C. Jacob, J. M. Starbuck, J. F. Fellers, S. Simunovic and R. G. Boeman, *J. Appl. Polym. Sci.*, 2004, **94**, 296–301.
58 X. Li and A. F. Yee, *Macromolecules*, 2004, **37**, 7231–7239.
59 D. Brown and J. H. R. Clarke, *Macromolecules*, 1991, **24**, 2075–2082.
60 M. Kitagawa, *J. Polym. Sci., Polym. Phys. Ed.*, 1977, **15**, 1601–1611.
61 L. M. Nicholson, *J. Mater. Sci.*, 2000, **5**, 6111–6121.
62 H. G. H. van Melick, L. E. Govaert and H. E. H. Meijer, *Polymer*, 2003, **44**, 2493–2502.
63 A. W. Christiansen, E. Baer and S. V. Radcliffe, *Philos. Mag.*, 1971, **24**, 451–467.
64 S. Rabinowitz, I. M. Ward and J. S. C. Parry, *J. Mater. Sci.*, 1970, **5**, 29–39.